Chemical Engineering Journal 427 (2022) 132050

Contents lists available at ScienceDirect

Chemical Engineering Journal

journal homepage: www.elsevier.com/locate/cej

Continuous removal of sulfate and metals from acidic mining-impacted waters at low temperature using a sulfate-reducing bacterial consortium

Hanna Virpiranta [a,*], Ville-Hermanni Sotaniemi [a], Tiina Leiviskä [a], Sanna Taskila [a], Jaakko Rämö [a], D. Barrie Johnson [b], Juha Tanskanen [a]

[a] University of Oulu, Chemical Process Engineering, PO Box 4300, 90014 Oulu, Finland
[b] Bangor University, School of Natural Sciences, Bangor LL57 2UW, United Kingdom & Coventry University, Health and Life Sciences, Coventry CV1 5FB, United Kingdom

ARTICLE INFO

Keywords:
Acid mine drainage
Bioreactor
Cold-tolerant sulfate-reducing bacteria
Metal removal
Sulfate removal

ABSTRACT

The aim of this study was to develop a biological method for the simultaneous removal of sulfate and metals from acidic low-temperature mining effluents. A mixed consortium of cold-tolerant sulfate-reducing bacteria (SRB) and other microorganisms was immobilized on glass beads and exploited in an up-flow biofilm reactor for the continuous treatment of actual and synthetic mining-impacted waters (MIWs) with initial sulfate concentrations between 1580 and 5350 mg L^{-1}. The proton acidity of the mine waters was neutralized by microbial sulfidogenesis. Metals present in the MIWs were precipitated either off-line or in-line, inside the reactor vessel. High sulfate reduction rates (SRRs), from 1000 to 4500 mg L^{-1} d^{-1} at a temperature of 11.7 ± 0.2 °C, were achieved (sulfate removal 43–87%). The bacterial consortium was found to be robust and resistant to changes in growth conditions during the bioreactor experiment. The relative abundance of SRB and the SRR increased at higher sulfate concentrations. Sulfidogenic bioreactors have the potential for treatment of acid mine drainage even at low temperature. It was demonstrated that neutral reactor conditions and high SRRs were maintained when acidic influent was fed into the reactor.

1. Introduction

Effluents from the mining industry are commonly characterized by having relatively elevated concentrations of soluble sulfate and transition metals, and are often moderately to extremely acidic [1,2]. As a result, these waters can cause pollution of ground and surface waters and decrease the biodiversity in fresh waters [3]. Consequently, there is a need to remove both metals and sulfate from such wastewaters before they are discharged into the environment.

Biological sulfate reduction is a widely-studied technology for remediating liquid waste streams that contain both sulfate and dissolved metals, especially at moderate temperature [4]. However, the most commonly used technology for sulfate removal is chemical precipitation with lime, which is suitable for high sulfate concentrations of several grams per liter, but the residual concentrations are from 1500 to 2000 mg L^{-1} and gypsum sludge is produced in large volumes [2,5]. Sulfate can also be removed from water by membrane filtration or ion exchange processes. These methods are efficient but have some disadvantages such as high costs, fouling of membranes, and the need for pre-precipitation of the water and downstream treatment of the reject [6]. Recently, biological treatment methods have been suggested for the removal of various contaminants [7] and the traditional bioreactors used for wastewater treatment have been developed significantly [8,9].

During growth, sulfate-reducing bacteria (SRB) convert sulfate to sulfide-S and oxidize organic carbon sources, preferably organic acids. The form of the produced sulfide-S is highly dependent on the pH of the environment [10]. At moderate temperature, and below pH 6.9, hydrogen sulfide (H_2S, a highly toxic and corrosive gas that can cause problems in industrial-scale applications [11]) is the dominant form, whereas hydrosulfide (HS^-) dominates in liquors between pH 7 and ~ 13. Sulfide (S^{2-}) combines with many monovalent and divalent metals to form insoluble sulfide phases, although the solubility products of metal sulfides are highly varied, resulting in some sulfides (such as copper and silver) forming in very low pH (<2) liquors, while others (such as manganese) only form in alkaline solutions. Sulfide precipitates are often more stable, more dense and less soluble than metal hydroxides

* Corresponding author.
E-mail address: hanna.virpiranta@oulu.fi (H. Virpiranta).

https://doi.org/10.1016/j.cej.2021.132050
Received 28 May 2021; Received in revised form 19 August 2021; Accepted 22 August 2021
Available online 26 August 2021

[10]. Therefore, many transition metals can readily be removed from contaminated waters as sulfide phases. In addition, sulfide precipitation results in very low metal concentrations and metal sulfides can be reused by smelting [11].

Most species of SRB grow in anaerobic environments with an optimal pH range from 5 to 8. However, there are also acidophilic and acid-tolerant strains, which can grow at lower pH values: sequences related to SRB have been found even at pH 1.4 [12]. Optimal bacterial growth conditions are usually essential for the efficient biological removal of pollutants from wastewaters. In northern areas of the world, microbial metabolism is often slow due to the cold climate. Nevertheless, by exploiting the native microbes of boreal areas and providing a suitable carbon source, sulfidogenesis can succeed even at low temperature [13]. It is important, therefore, to develop an efficient sulfate reduction method for cold conditions since several mines that generate sulfate- and metal-rich wastewaters operate in the Arctic and subarctic regions, e.g., in Canada [14], Finland [15], and Norway [16].

Previously reported low-temperature (<20 °C) sulfate reduction reactor studies are listed in Table 1. Semi-passive and passive treatments were tested in anaerobic columns filled with spent horse manure by Tsukamoto et al. [17], in a packed bed reactor filled with waste rocks 20% by volume by Nielsen et al. [13], and in a column reactor filled with a mixture consisting of wood chips, leaf compost, ash, sand, and municipal sludge, which acted as both a carbon source and an SRB inoculum, by Ben Ali et al. [18]. Active reactors operated at low temperature include a fluidized-bed reactor filled with silica mineral as a biomass carrier [19] and a submerged membrane bioreactor [20]. Treatment of mining wastewaters with sulfate concentrations higher than 2 g L^{-1} has previously been reported at low temperature only by Nevatalo et al. [20].

Although extensive research has been carried out on sulfate-reducing bioreactors, most previous low-temperature reactor studies have been conducted with synthetic mine waters (SMWs) containing moderate sulfate concentrations (up to 2 g L^{-1}: ~21 mM). There is a need to perform studies using conditions that more accurately reflect those in the environment and to develop solutions for comprehensive metal and sulfate removal in mining-impacted waters (MIWs). The current study seems to be the first description of the treatment of actual acid mine drainage (AMD: with sulfate concentrations > 1 g L^{-1}) as well as that of actual jarosite-contaminated water (JCW: with sulfate concentrations > 4 g L^{-1}) at low temperature. This study also provides valuable information on in-line and off-line removal of metals by H_2S precipitation. In addition, investigation of the SRB consortium by 16S rRNA gene sequencing provides new information on the effect of higher metal and sulfate concentrations in actual MIWs on the SRB consortium.

2. Materials and methods

2.1. Low-temperature sulfidogenic up-flow biofilm reactor

Biological sulfate reduction was investigated at a temperature of 11.7 ± 0.2 °C in a continuous-flow bioreactor (Applikon Biotechnology, U.S.) with a working volume of 1.8 L (liquid volume 1.2 L), operated as an up-flow biofilm system, as described by Ñancucheo and Johnson [21] (Fig. 1). The reactor was connected to a Biostat C unit (B. Braun Biotech International GmbH, Germany) to control the pH and liquid level. Agitation (50 rpm) using a Rushton turbine located within the top liquid layer was controlled with an ADI 1012 motor controller (Applikon Biotechnology, U.S.). The reactor temperature was controlled with a circulating water–ethanol mixture inside the reactor jacket, using a refrigerated circulating bath (VWR International, U.S.). The reactor was maintained at near-neutral pH (7.0–7.5) under anaerobic conditions. At the beginning of the experiment, the reactor was operated in batch mode for two weeks to increase the sulfate reduction rate (SRR) and number of SRB. This was followed by a continuous flow of sulfate-rich water into and out of the reactor vessel. The flow rate was varied to maintain the pH within the reactor vessel. Sulfate reduction caused the pH to increase, and acidic MIW (pH 2.7–3.3) was fed into the reactor via an L-shaped perforated tube to maintain the pH at the set range of 7.0–7.5. The liquid surface level was controlled by a liquid level sensor connected to an outflow pump and a drain tube placed below the liquid surface. The bacteria were immobilized on 1–2 mm diameter porous glass beads (DennertPoraver GmbH, Germany) to help to retain them within the reactor vessel. The volume of beads in the reactor was 0.6 L. A continuous nitrogen gas flow was used to replace any oxygen inside the reactor and to flush the formed H_2S gas out of the reactor. The H_2S gas generated was used to precipitate the metals: gas was routed from the reactor into a separate metal solution, either synthetic $CuSO_4$ (J.T.Baker) solution or actual MIWs. The precipitated metal solutions were vacuum filtered through a 1.2 μm glass fiber filter and the precipitates dried at 60 °C and weighed. The filtered MIWs were used as the reactor feed.

The SRB consortium used in this study was enriched from an Arctic sediment sample from northern Finland, described in a previous study [22]. The consortium was cold-acclimated and characterized by 16S rRNA sequencing. Approximately 19% of the bacteria were found to be SRB, most of them belonging to the genus *Desulfobulbus*. The consortium

Table 1
Reported low-temperature sulfate reduction bioreactor experiments.

Reactor type	Treated water	Electron donor	COD/ SO_4^{2-}	Temperature (°C)	Influent pH	Influent SO_4^{2-} (mg L^{-1})	HRT	SRR(mg L^{-1} d^{-1})	SO_4^{2-} removal (%)	Reference
column	SMW	ethanol	1.0	5–15	4.2	900	6.6 h	1400 ± 400	44 ± 11	[17]
column	SMW	methanol	1.0	5–15	4.2	900	6.6 h	1300 ± 400	39 ± 12	[17]
FBR	SMW	ethanol	2.0	8	5–7	1000	1 d	260 ± 30	35 ± 4	[19]
MBR	SMW	H_2	4.0	9	7.5	2880	6 d	300 ± 300	60	[20]
MBR	SMW	H_2	4.0	9	7.5	3460	6 d	300 ± 300	50	[20]
MBR	SMW	H_2	4.0	9	7.5	5760	6 d	400 ± 100	40	[20]
PBR	NMD	molasses	n.d.	4–17	6.8 ± 0.5	420 ± 140	2 w	0–28	0–92	[13]
column	SMW	wood chips, leaf compost	n.d.	5	2.8–3.5	1610 ± 130	2.5 or 5 d	< 260	<40	[18]
UBR	SMW	succinic acid, YE	0.8	11.7 ± 0.2	3.1 ± 0.1	1580 ± 90	16 ± 6 h	1950 ± 950	51 ± 11	This study
UBR	AMD	succinic acid, YE	0.8	11.7 ± 0.2	3.3 ± 0.1	1260 ± 60	14 ± 5 h	1575 ± 445	43 ± 6	This study
UBR	JCW	succinic acid, YE	0.8	11.7 ± 0.2	2.8 ± 0.1	4400 ± 200	31 ± 8 h	3400 ± 1100	65 ± 7	This study
UBR	JCW	succinic acid, YE	1.4	11.7 ± 0.2	2.7 ± 0.0	4200 ± 200	34 ± 6 h	3900 ± 400	87 ± 8	This study

AMD – acid mine drainage, FBR – fluidized bed reactor, HRT – hydraulic retention time, JCW – jarosite-contaminated water, MBR – membrane bioreactor, n.d. – not determined, NMD – neutral mine drainage, PBR – packed bed reactor, SMW – synthetic mine water, SRR – sulfate reduction rate, UBR – up-flow biofilm reactor, YE – yeast extract.

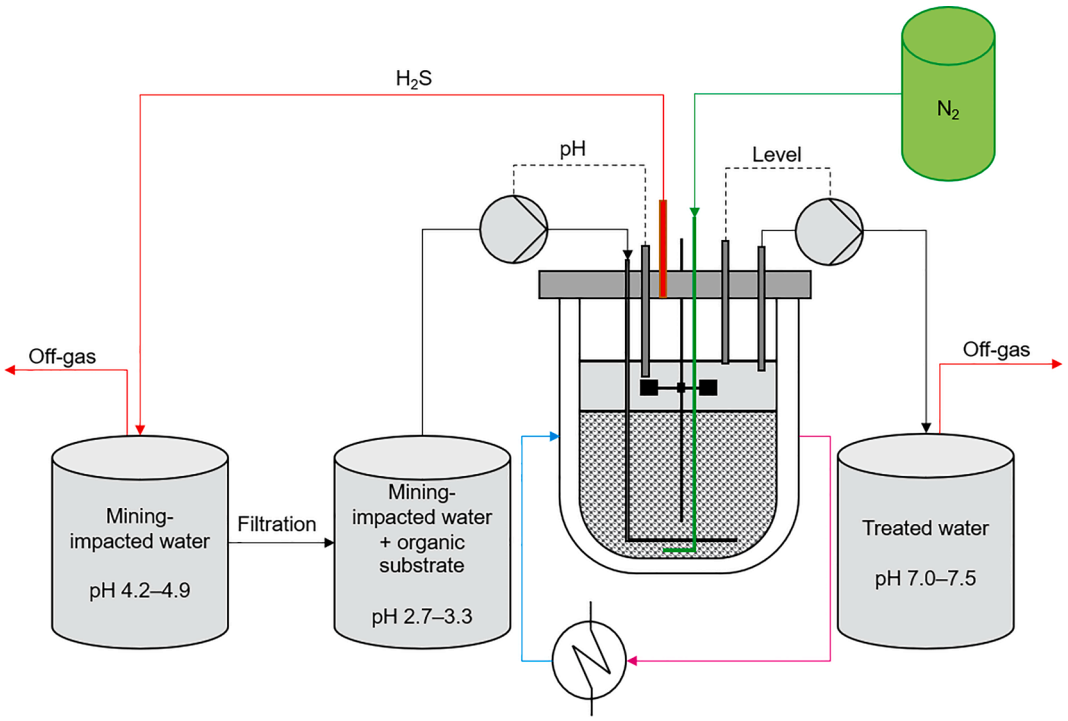

Fig. 1. Design of the sulfidogenic up-flow biofilm reactor used for treatment of actual MIWs at low temperature. When acidic SMW was treated, the H_2S gas produced in the reactor was routed into synthetic $CuSO_4$ solution.

was able to reduce sulfate at a temperature of 6 °C with succinate as the electron donor.

The inoculant for the bioreactor was enriched by incubating 50 mL of the sterile glass beads with the SRB consortium for six weeks at 6 °C. SMW with succinate as a carbon source was used as the cultivation medium. The components of the SMW (1.0 g Na_2SO_4 (Merck), 0.1 g $CaSO_4{\cdot}2H_2O$ (Merck), 2.0 g $MgSO_4{\cdot}7H_2O$ (VWR), 0.5 g K_2SO_4 (VWR), 0.2 g ascorbic acid (VWR), 0.34 g NH_4Cl (VWR), 0.07 g K_2HPO_4 (Merck), 0.1 g yeast extract (Honeywell Fluka) L^{-1}), with the exception of $FeSO_4{\cdot}7H_2O$ (J.T.Baker) and sodium succinate (Merck), were dissolved in deionized water. Before autoclaving at 121 °C for 20 min, the pH of the water was adjusted to 7.8 with NaOH and the solution poured into a 250 mL glass bottle containing 50 mL of glass beads. The bottle was sealed with a screw cap with a septum, and after autoclaving and cooling to 6 °C, $FeSO_4$ and sodium succinate solutions were added aseptically to give iron and succinate concentrations of 0.10 g L^{-1} and 1.75 g L^{-1}, respectively. All the chemicals used in the media were of analytical grade.

2.2. Mining-impacted waters

The sulfidogenic bioreactor was used for the treatment of three different MIWs containing sulfate and metals: an acidic SMW, as well as an actual AMD, and JCW collected from closed Finnish mine sites (Table 2). Succinic acid (VWR) as a carbon source and other nutrients (0.15 g NH_4Cl, 0.05 g K_2HPO_4, 0.1 g yeast extract L^{-1}) were added to the water before it was fed into the reactor. For each type of water tested, a chemical oxygen demand (COD)/sulfate ratio of 0.8 was used. Also, a higher COD/sulfate ratio of 1.4 was tested using the JWC with the highest initial sulfate concentration. Since succinic acid had already been found suitable for the SRB consortium [22], it was used as a carbon and energy source throughout the bioreactor experiments. Due to the high aluminum concentration in the AMD, it was first precipitated by increasing the pH to 6.0 ± 0.2 with 5 M NaOH (VWR) solution. In addition, both actual MIWs were precipitated with the H_2S formed in the reactor. Precipitation with H_2S alone was also tested for the AMD to examine the effect of H_2S on metal precipitation. After precipitation, filtration, and nutrient addition, the initial sulfate concentrations of the acidic SMW, AMD, and JCW at COD/SO_4^{2-} ratios of 0.8 and 1.4 were 1580 ± 90 mg L^{-1}, 1260 ± 60 mg L^{-1}, 4400 ± 200 mg L^{-1}, and 4200 ±

Table 2
Characteristics of MIWs.

Analyte	SMW	AMD	JCW
pH	3.1	4.2	4.9
COD (mg L^{-1})	–	23	52
Chloride (mg L^{-1})	99	15	1 200
Fluoride (mg L^{-1})	–	26	0.68
Sulfate (mg L^{-1})	1 580	1 600	5 350
Nitrate (mg L^{-1})	–	66	0.18
Nitrite (μg L^{-1})	–	< 7	120
Ammonium (mg L^{-1})	51	0.62	6.1
Phosphate (mg L^{-1})	27	0.034	0.021
Aluminum (mg L^{-1})	–	68	1.4
Antimony (μg L^{-1})	–	< 0.5	< 0.25
Arsenic (μg L^{-1})	–	< 0.5	3.2
Boron (μg L^{-1})	–	30	350
Barium (μg L^{-1})	–	16	53
Beryllium (μg L^{-1})	–	4.7	0.26
Cadmium (μg L^{-1})	–	42	56
Cobalt (mg L^{-1})	–	0.23	10
Chromium (μg L^{-1})	–	2.3	5.4
Copper (mg L^{-1})	–	0.9	0.1
Iron (mg L^{-1})	5	2	200
Lead (μg L^{-1})	–	28	8.3
Manganese (mg L^{-1})	–	9.5	6.1
Mercury (μg L^{-1})	–	< 0.2	< 0.1
Molybdenum (μg L^{-1})	–	< 0.5	0.44
Nickel (mg L^{-1})	–	0.1	20
Selenium (μg L^{-1})	–	< 2	1.1
Strontium (mg L^{-1})	–	0.56	1.2
Thallium (μg L^{-1})		0.17	< 0.05
Tin (μg L^{-1})	–	< 0.5	< 0.25
Uranium (μg L^{-1})	–	41	0.85
Vanadium (μg L^{-1})	–	1.4	3.4
Zinc (mg L^{-1})	–	14	1.9

200 mg L^{-1}, respectively. The corresponding pH values of the feed liquids were 3.1 ± 0.1, 3.3 ± 0.1, 2.8 ± 0.1, and 2.7 ± 0.0. The characteristics of the MIWs and operational parameters of the sulfidogenic bioreactor during the experiments are listed in Supplementary Table S1.

2.3. Sampling and analysis

Samples were collected periodically from the reactor liquid through a valve with a syringe and filtered through a 0.22 μm syringe filter. The redox potential and sulfate concentration were measured from the filtrate. An IQ150 pH Dual Technology meter equipped with a pHenomenal ORP220 Ag/AgCl (3 M KCl) electrode was used for measuring the redox potential. For reference to a standard hydrogen electrode, +215 mV (AgCl/Ag potential at 10 °C) was added to the recorded redox potentials [23]. The Hach Lange Sulfate cuvette test LCK 353 and a UV/Vis Spectrophotometer DR 2800 were used for determining the sulfate concentrations. Succinate, acetate, and propionate concentrations were analyzed by high-performance liquid chromatography (HPLC) using a diode-array detector (DAD). The detection wavelength was set at 280 nm. The compounds were separated on an IC Sep ICE-Coregel 87H3 column (Transgenomic Inc. U.S.) at 60 °C with 0.005 M H_2SO_4 (Merck) solution in water as a mobile phase. The flow rate and injection volume were 0.8 mL min^{-1} and 10 μL, respectively. A theoretical amount of acetate produced was calculated according to the reaction stoichiometry (Eq. (1)), assuming that all the succinate consumed was used for sulfate reduction.

$$4(CH_2)_2(COOH)_2 + 3SO_4^{2-} + 2H^+ \rightarrow 4CH_3COO^- + 3H_2S + 8CO_2 + 4H_2O \quad (1)$$

The chemical oxygen demand (COD) values of the raw actual MIWs were measured using the Hach Lange COD cuvette test LCK 314. The analysis of anions in the raw and treated actual MIWs was performed as follows: Cl^-, F^-, and SO_4^{2-} were analyzed using ion chromatography (SFS-EN ISO 10304–1:2009) and NO_2-N, NO_3-N, NH_4-N, and PO_4-P were analyzed using a continuous flow analyzer (SFS-EN ISO 13395:1997, SFS-EN ISO 11732:2005, SFS-EN ISO 15681–2:2005) or a discrete analyzer (ISO 15923–1:2013). The elemental analysis was conducted using inductively coupled plasma mass spectrometry (ICP-MS) (SFS-EN ISO 17294–2:2016) or nitric acid digestion for the extraction of trace elements (SFS-EN ISO 15587–2:2002). Version 5.0 of the MINEQL+ program [24] was used for chemical equilibrium calculations to model the formation of mineral phases during the precipitation of synthetic $CuSO_4$ solution and MIWs, as well as inside the sulfidogenic bioreactor.

X-ray photoelectron spectroscopy (XPS) and X-ray diffraction (XRD) were used for the characterization of metal precipitates collected by filtration after the precipitation of MIWs and $CuSO_4$ solution. The XRD patterns were obtained using a Rikagu SmartLab rotating anode diffractometer (Tokyo, Japan) with Cu-Kβ radiation in the range of 5–130°2θ (0.02°2θ step). The XPS spectra were recorded with a Thermo Fisher Scientific ESCALAB 250Xi spectrometer (Waltham, U.S.) using monochromatic Al Kα radiation (1486.6 eV). The charge calibration was performed by setting the binding energy of adventitious carbon to 284.8 eV.

Samples for the 16S rRNA sequencing analysis were taken at the end of each experiment with the various feed liquids. Samples were withdrawn aseptically from three different levels: the bottom of the bead layer, middle of the bead layer, and top liquid layer. The genomic DNA of the microbial strains was isolated from the cell pellets using the standard protocol [25]. The SRB consortia were characterized by 16S rRNA sequencing at the Biocenter Oulu Sequencing Center, as described previously in Virpiranta et al. [22]. The obtained sequences were compared with those present in GenBank using a BLAST tool (National Center for Biotechnology Information, U.S. National Library of Medicine, U.S.). The richness and alpha diversity of the bacterial species were evaluated using species richness (S); the Shannon diversity index (H) described in Eq. (2), where p_i is the proportion of the i^{th} species; and true diversity, i.e., the effective number of the species (ENS) described in Eq. (3):

$$H = -\sum_{i=1}^{S} p_i \ln p_i \quad (2)$$

$$ENS = e^H \quad (3)$$

3. Results

3.1. Sulfate removal

Sulfate reduction was evidenced soon after continuous flow commenced by the precipitation of black CuS in the gas jar that received the off-gas produced in the bioreactor. Approximately half of the sulfate present was reduced in the reactor during the treatment of both AMD and acidic SMW with initial sulfate concentrations of 1260 and 1580 mg L^{-1}, respectively (Fig. 2). In the case of JCW, approximately two-thirds of the initial sulfate concentration of 4400 mg L^{-1} was reduced at the COD/SO_4^{2-} ratio of 0.8. The highest removal rate, 87%, was achieved at the COD/SO_4^{2-} ratio of 1.4 during the treatment of JCW with an initial sulfate concentration of 4200 mg L^{-1}.

At the different operational pH values, the feed rate as well as the SRR varied considerably, reaching the highest rates at the lowest pH (7.00 ± 0.10) (Figs. 2 and 3). The different operational pH values did not have any significant effect on the residual sulfate concentration of the treated water. In the case of acidic SMW, the hydraulic retention time (HRT) increased from around 13 h to 21 h when the operational pH value was increased from 7.00 to 7.25. In the case of AMD, the HRT was 10 h and 18 h at the operational pH values of 7.25 and 7.50, respectively. When JCW was treated at the COD/SO_4^{2-} ratio of 0.8, the HRT increased from 26 h to 34 h and further to 38 h, at the operational pH values of 7.00, 7.25, and 7.50, respectively. At the COD/SO_4^{2-} ratio of 1.4, the HRT was around 34 h at a pH value of 7.00. The highest SRR achieved was 4200 ± 300 mg L^{-1} d^{-1}, when JCW was treated. In this case, the residual sulfate concentration remained at around 1600 mg L^{-1} at the COD/SO_4^{2-} ratio of 0.8, but a residual concentration of 560 mg L^{-1} was achieved at the COD/SO_4^{2-} ratio of 1.4. However, the SRR decreased to 3900 mg L^{-1} d^{-1} at the COD/SO_4^{2-} ratio of 1.4.

During the treatment of acidic SMW, the E_H within the bioreactor remained at around 0 mV regardless of the operational pH, whereas during the treatment of actual MIWs the E_H decreased to < 0 and was more negative at higher operational pH values. The redox potential values (E_H) are listed in the supplementary material (Table S2).

3.2. Metal and metalloid removal

The most dramatic drop in metal concentrations in the actual MIWs after precipitation and sulfate reduction was detected for aluminum, cobalt, copper, iron, nickel, and zinc (Table 3). Most of the metals were precipitated with H_2S or NaOH before the MIW was fed into the reactor. However, according to the elemental analyses of the MIWs, cobalt and nickel in particular precipitated mostly inside the sulfidogenic bioreactor (Table 3). There was no significant difference in metal removal between the COD/SO_4^{2-} ratios of 0.8 and 1.4 used in the treatment of JCW. Detailed characteristics of the treated waters are presented in the supplementary material (Table S3).

The metals identified from the recovered precipitates by XPS analysis were aluminum, copper, cobalt, iron, and zinc (Table 4). The aluminum in the actual MIWs had probably formed hydroxide precipitates before the actual MIWs were precipitated with H_2S or NaOH and was therefore also removed by filtration after H_2S precipitation. Copper was detected only in the precipitate collected from the synthetic $CuSO_4$ solution. Chemical speciation calculations made with the MINEQL+ program estimated that copper precipitated totally as covellite (CuS) (Table S4).

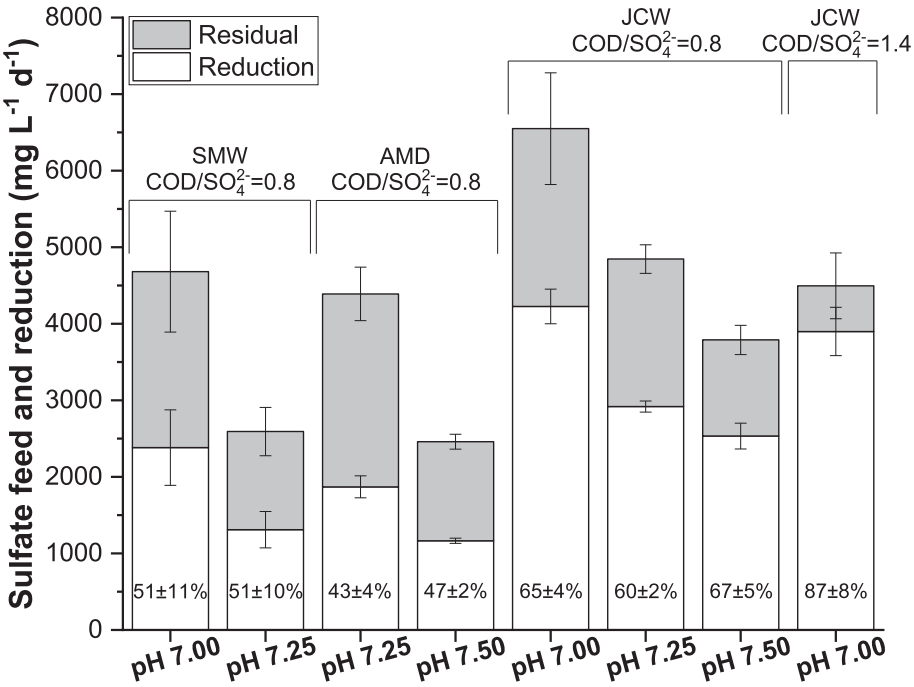

Fig. 2. Sulfate feed (whole bar) and reduction (white bar) with removal % during treatment of acidic SMW, AMD, and JCW at different operational pHs and COD/SO_4^{2-} ratios. Averaged values of daily measurements with standard deviations are shown.

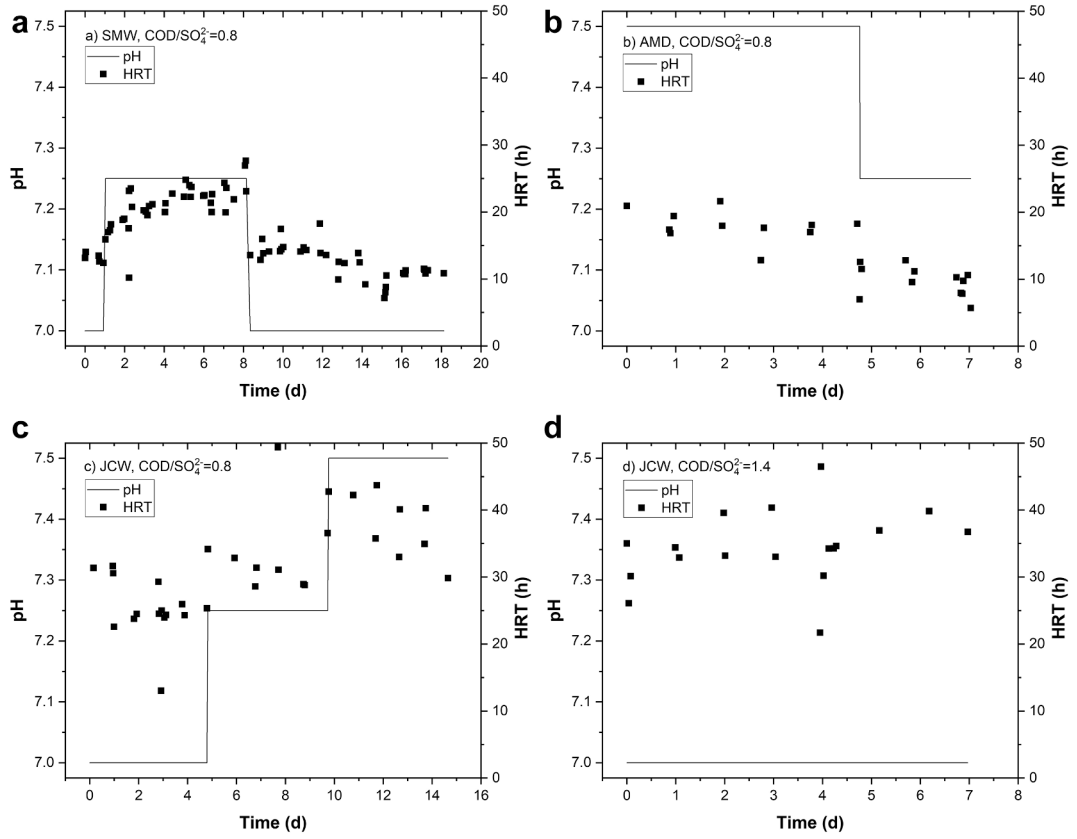

Fig. 3. Effect of operational pH on hydraulic retention time (HRT) in the sulfidogenic bioreactor during treatment of a) SMW (feed pH 3.1 ± 0.1), b) AMD (feed pH 3.3 ± 0.1), and JCW at COD/SO_4^{2-} ratios of c) 0.8 (feed pH 2.8 ± 0.1) and d) 1.4 (feed pH 2.7 ± 0.0).

However, the XRD data indicated the presence of both $CuSO_4$ and CuS in the precipitate (Fig. S1a), which was further supported by XPS analysis. The high-resolution S2p XPS spectrum shows a major component at 169.0 eV ($S2p_{3/2}$) and a minor component at 162.5 eV ($S2p_{3/2}$) binding energies (Fig. S2a), which can be attributed to sulfate and sulfide, respectively [26]. The Cu2p high-resolution spectrum has $Cu2p_{3/2}$ peaks

Table 3
Removal of metals and metalloids from actual MIWs by filtration. The removal % is calculated according to the initial concentrations in the actual MIWs.

Treatment	Precipitation with H_2S	Precipitation with NaOH and H_2S	Sulfate reduction, pH 7.25 ± 0.10	Precipitation with H_2S	Sulfate reduction, pH 7.00 ± 0.10
Removal (wt.%)	AMD	AMD	AMD	JCW	JCW
Aluminum	82*	99	1	72*	21
Arsenic	0	0	0	16	53
Boron	0	0	0	9	0
Barium	0	0	0	2	15
Beryllium	0	79	0	0	0
Cadmium	82	99	> 0	87	13
Cobalt	0	22	77	19	80
Copper	98	100	0	53	45
Iron	59	97	> 0	30	70
Lead	84	> 99	0	> 88	> 7
Manganese	0	9	2	3	0
Nickel	0	22	60	15	83
Strontium	0	9	0	0	17
Uranium	0	96	2	26	46
Zinc	14	99	1	47	52

* Not as a sulfide phase.

Table 4
Surface composition (wt.%) of the metal precipitates recovered by filtration after precipitation of synthetic $CuSO_4$ solution, AMD, and JCW.

Water treated	Precipitant	Cu (%)	Zn (%)	Fe (%)	Co (%)	Al (%)	Ca (%)	Mg (%)	F (%)	Si (%)	S (%)	O (%)	C (%)
$CuSO_4$ solution	H_2S	36.9	–	–	–	–	–	–	–	–	22.9	39.0	1.2
AMD	5 M NaOH*	–	3.7	–	–	30.0	1.3	0.7	9.4	2.7	3.8	44.1	4.4
AMD	H_2S**	–	49.9	–	–	–	–	–	–	10.4	24.3	13.5	1.9
JCW	H_2S***	–	3.2	24.4	4.5	6.6	–	–	3.3	1.9	10.0	38.7	7.3

* Small amounts of Fe, Ni, and Cu were also found according to the high-resolution spectra.
** Small amounts of Fe, Al, and Co were also found according to the high-resolution spectra.
*** Small amounts of Cu and Ni were also found according to the high-resolution spectra; inaccurate Co amount.

at around 932 eV and 935 eV, along with strong satellite features. The peak at 935 eV coincides with the $CuSO_4$ peak position [27]. CuS has a $Cu2p_{3/2}$ peak at 932.2 ± 0.2 eV [27], and thus is in line with the observed peak in this study. However, Cu2p has small chemical shifts for copper species such as CuS, CuS_2, and Cu_2O, and thus they are difficult to differentiate using the Cu2p spectrum alone. Nevertheless, the satellite peaks confirm the presence of Cu(II) in the precipitate [26,27].

The precipitate collected after the NaOH precipitation of AMD consisted mostly of aluminum, but also significant amounts of fluorine, some zinc, and sulfur were observed (Table 4). Chemical speciation calculations estimated the precipitation of aluminum as diaspore (AlO(OH)) (Table S4). However, this is unlikely, since XRD indicated that the precipitate was amorphous in nature (Fig. S1b). Precipitation of aluminum as hydroxides or hydroxy sulfates is more probable [28]. Fluoride was probably mostly co-precipitated with aluminum, which is supported by the peak in the Al2p XPS spectrum as a result of Al–F bonding that is wider than that reported for pure aluminum hydroxide [29,30]. The Zn2p high-resolution XPS spectrum show two $Zn2p_{3/2}$ peaks at around 1021.6 eV and 1026.5 eV. The peak at the lower BE might be mostly related to $Zn(OH)_2$ [31], but other zinc compounds (e.g. ZnO, ZnS) cannot be excluded. The $Zn2p_{3/2}$ peak at the higher BE might be attributed to some spinel structure with Zn [32]. The S2p spectrum was fitted to three doublets, and most of the sulfur was present in sulfate form ($S2p_{3/2}$ peak at 169.1 eV, Fig. S2b). The minor components probably correspond to sulfite ($S2p_{3/2}$ peak at 167.8 eV) [33] and sulfide ($S2p_{3/2}$ peak at 162.9 eV). Small amounts of iron, nickel, and copper were detected according to the XPS high-resolution spectra (Fig. S3a). Chemical speciation calculations estimated that iron would precipitate mostly as hematite (Fe_2O_3), but also as cobalt ferrite ($CoFe_2O_4$). Removal of the detected metals cannot be confirmed by elemental analysis results since the quality of the AMD was not analyzed after the NaOH precipitation.

Zinc was the only metal detected in the precipitate collected after the H_2S precipitation of AMD (Table 4) and XRD indicated the presence of zinc sulfide (Fig. S1c), which was consistent with the S2p and Zn2p high-resolution XPS spectra. Sulfur was in sulfide form and the $S2p_{3/2}$ peak was located at 162.2 eV (Fig. S2c). In the Zn2p spectrum, two $Zn2p_{3/2}$ peaks were observed, a major peak located at around 1022 eV and a minor peak located at around 1024 eV, both of which can probably be attributed to ZnS [34]. Small amounts of iron, aluminum, and cobalt were also found according to the XPS high-resolution spectra (Fig. S3b).

The bulk of the metal precipitated from JCW was iron. Chemical speciation calculations estimated that iron would precipitate as akageneite ($Fe(OH)_{2.7}Cl_{0.3}$) and cobalt ferrite ($CoFe_2O_4$), whereas it was estimated that aluminum would precipitate as alunite ($KAl_3(SO_4)_2(OH)_6$) (Table S4). In addition, the calculations suggested that zinc would remain dissolved. XRD analysis showed the formation of both amorphous precipitate and the presence of elemental sulfur (Fig. S1d). The XPS analysis of the precipitate showed a high amount of iron and the $Fe2p_{3/2}$ peak was located at around 711 eV, which might be related to goethite [35]. The $Fe2p_{3/2}$ peaks of jarosite and akageneite have been found at 712.0 eV [36] and 712.4 eV [37], respectively. On the other hand, cobalt ferrite has been reported to have a $Fe2p_{3/2}$ peak at 710.2 eV, while the BE increased with decreased Co content [38]. The Co2p spectrum showed a $Co2p_{3/2}$ peak at ~ 780.3 eV and intense satellite peaks, indicating the Co(II) state [39]. The S2p spectrum indicates the presence of at least three sulfur species (Fig. S2d). The sulfate peak is located at 168.7 eV ($S2p_{3/2}$). The sulfide peak at the lower binding energy is wide and consists of two doublets with $S2p_{3/2}$ peaks at 161.7 eV and 163.2 eV, indicating the presence of different sulfide species. Elemental sulfur might also have been present, although the $S2p_{3/2}$ peak of elemental sulfur is located at a slightly higher BE (164.3 eV) [40]. A $Zn2p_{3/2}$ peak is visible at 1021.8 eV, probably originating from ZnS [34]. In addition, small amounts of copper and nickel were detected according to the XPS high-resolution spectra (Fig. S3c).

Inside the reactor, the chemical speciation calculations estimated that iron, cobalt, copper, nickel, and zinc would be precipitated as pyrite (FeS_2), jaipurite (CoS), chalcopyrite ($CuFeS_2$) or CuS, millerite (NiS), and sphalerite ((Zn, Fe)S), respectively. The solubility of the metals was influenced by both the E_H and pH of the reactor. The calculations

suggested that, in AMD and SMW, most of the transition metals were dissolved and flowed through the reactor at pH values of 7.00, 7.25, and 7.50 with an E_H higher than –140 mV, –150 mV, and –160 mV, respectively. In JCW, the metal concentrations were higher, and the metals started to precipitate at higher E_H. The aluminum in AMD was totally precipitated as diaspore (AlO(OH)) at pH values of 7.25 and 7.50, despite the E_H. At pH 7.50, the aluminum in JCW precipitated as diaspore when the E_H was –165 mV or lower, and as hercynite ($FeAl_2O_4$) when the E_H was –160 mV or higher. At pH values of 7.00 and 7.25, the aluminum in JCW precipitated only as diaspore. The estimated dependence of the solubility of the metals on the E_H at different operational pH values during the treatment of MIWs is shown in the supplementary material (Figs. S4–S6).

3.3. Analysis of organic acids

Concentrations of residual succinate, propionate, and acetate (produced by the incomplete oxidation of succinate) and the theoretical concentrations of acetate are shown in Fig. 4. In all of the experiments at the COD/SO_4^{2-} ratio of 0.8, the effluent succinate concentration was close to 0 mg L^{-1} throughout the tests. However, when JCW was treated at the COD/SO_4^{2-} ratio of 1.4, approximately 300 mg L^{-1} of succinate remained.

Assuming that (i) all of the succinate consumed in the reactor was utilized for sulfate reduction and (ii) all of this was incompletely oxidized to CO_2 and acetate (Eq. (1)), then stoichiometric amounts of acetate should have been generated which, unless oxidized further by members of the microbial community in the bioreactor, would have been detected in the effluent liquors. The theoretical amount of acetate was close to the real amount of effluent acetate with all the waters treated at the COD/SO_4^{2-} ratio of 0.8. However, at the higher ratio of 1.4 in the case of JCW, the concentration of acetate was approximately 600 mg L^{-1} lower than the theoretical amount. In addition, some propionate was produced in all of the experiments. The propionate concentration was similar to that of the residual succinate in all of the experiments.

3.4. Characterization of the sulfate-reducing bacterial consortium

Approximately 55 different bacterial species in total were detected in the samples taken from the sulfidogenic bioreactor at the end of the sulfate reduction experiments (Table 5). The numbers of bacteria were greater in the samples taken from the middle of the bead layer than in the bottom and top layers. In addition, the Shannon diversity index and the ENS were the lowest in the samples taken after treatment of JCW at the COD/SO_4^{2-} ratio of 0.8. The highest species richness was observed after the treatment of JCW at the COD/SO_4^{2-} ratio of 1.4, while the highest Shannon diversity index and ENS values were detected after the treatment of acidic SMW.

The bacterial consortium cultivated in the reactor consisted mostly of Proteobacteria, Firmicutes, and Bacteroidetes. The relative abundance of Firmicutes was highest in the samples taken from the bottom of

Table 5
Species richness, Shannon diversity index, and effective number of species (ENS) in the sulfidogenic bioreactor after treatment of acidic SMW, AMD, and JCW at COD/SO_4^{2-} ratios of 0.8 and 1.4. Averaged values of three samples taken from the top, middle, and bottom layers of the reactor with standard deviations are shown.

Treated water	COD/SO_4^{2-} ratio	Species richness	Shannon diversity index	ENS
SMW	0.8	57 ± 8	2.55 ± 0.10	12.9 ± 1.2
AMD	0.8	54 ± 3	2.51 ± 0.05	12.3 ± 0.6
JCW	0.8	51 ± 6	2.00 ± 0.30	7.0 ± 3.0
JCW	1.4	58 ± 5	2.21 ± 0.15	9.2 ± 1.4

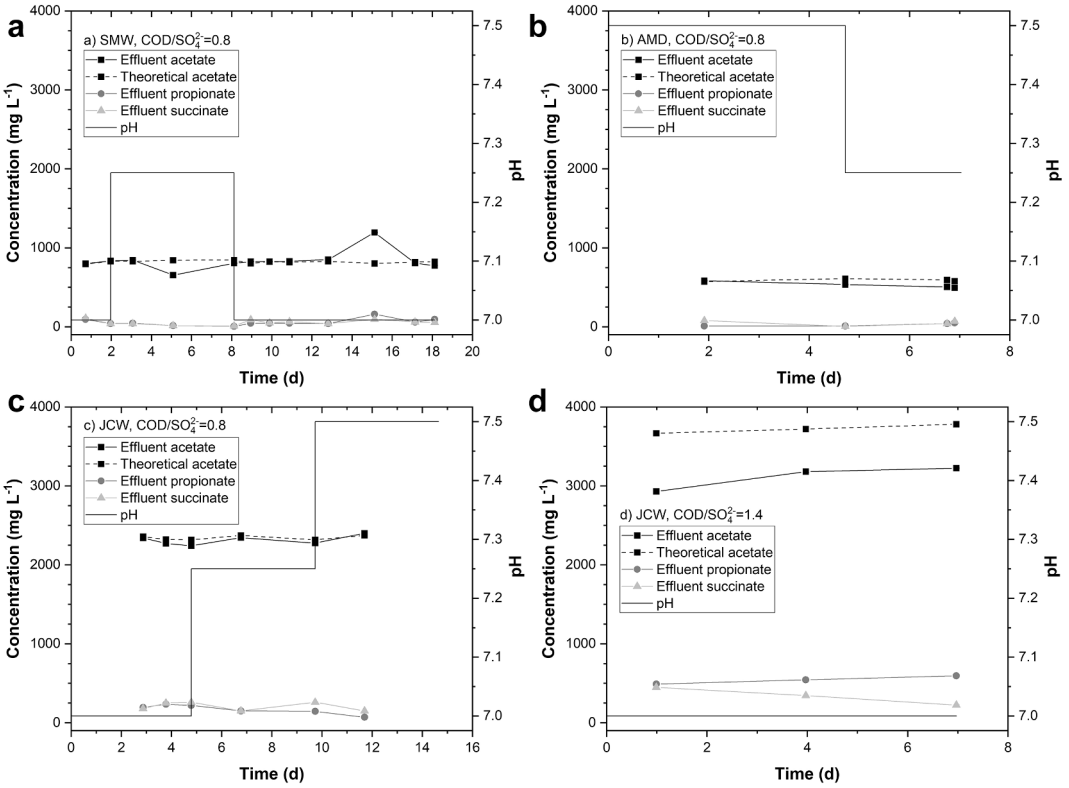

Fig. 4. Residual succinate concentrations (light gray triangles), propionate produced (dark gray circles), acetate produced (black squares), and theoretical acetate (black squares and dashed line) calculated according to the succinate concentrations utilized during the treatment of a) acidic SMW, b) AMD, and JCW at COD/SO_4^{2-} ratios of c) 0.8 and d) 1.4.

the reactor, whereas Proteobacteria were dominant in the samples taken from the top liquid layer and from the middle of the bead layer. The relative abundance of Proteobacteria was also highest after the treatment of AMD and JCW at the COD/SO_4^{2-} ratio of 1.4. Firmicutes and Bacteroidetes were more dominant after the treatment of acidic SMW and JCW, respectively, at the COD/SO_4^{2-} ratio of 0.8.

The relative abundance of SRB was highest in the samples taken from the top liquid layer of the reactor and in the samples taken after the treatment of JCW at the COD/SO_4^{2-} ratio of 1.4, when the approximate abundance was 38 ± 12% of the total bacteria. After the treatment of JCW, AMD, and acidic SMW at the COD/SO_4^{2-} ratio of 0.8, the relative abundance of SRB was 17 ± 10%, 15 ± 4%, and 8 ± 5%, respectively. Most of the SRB were characterized as *Desulfobulbus* sp. (Deltaproteobacteria), although some *Desulfovibrio* sp. (Deltaproteobacteria) and *Peptococcaceae* (Firmicutes) were also present. The only identified species belonging to the family *Peptococcaceae* among the cultivated consortium was *Desulfurispora* sp. The relative abundance of the SRB is presented in Fig. 5. Species richness at different sequencing depths as well as SRB distribution expressed as the number of sequence reads are presented in the supplementary material (Figs. S7–S8).

Other bacteria present in the reactor, some of which are involved in the cycling of sulfur, were *Arcobacter* sp., *Geobacter* sp., and *Halothiobacillus* sp. *Arcobacter* sp. was found mostly after the treatment of AMD, but not after the treatment of JCW. The relative abundance after the treatment of AMD and acidic SMW was 9 ± 4% and 4.0 ± 0.9%, respectively. Both *Geobacter* sp. and *Halothiobacillus* sp. were most abundant after the treatment of AMD: the relative abundance was 16 ± 2% and 15 ± 5%, respectively. With the other treated MIWs, the proportion of *Geobacter* sp. was <10%. The relative abundance of *Halothiobacillus* sp. was clearly lowest after the treatment of JCW: 4.7 ± 1.4% and 1.0 ± 1.0% at COD/SO_4^{2-} ratios of 0.8 and 1.4, respectively. After the treatment of acidic SMW, the relative abundance of *Halothiobacillus* sp. was 8 ± 4%, and both *Geobacter* sp. and *Halothiobacillus* sp. were least abundant at the bottom of the reactor. In addition, 3–13% of the bacterial consortium consisted of *Proteiniclasticum* sp, which was present at all levels of the reactor after the treatment of each MIW.

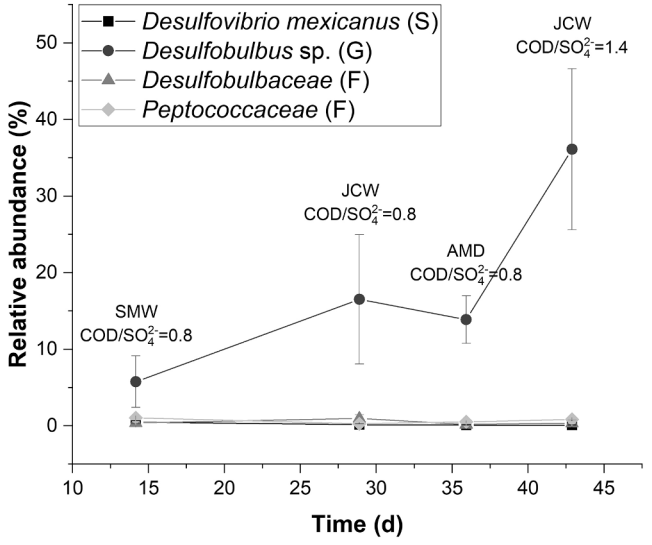

Fig. 5. Relative abundance of SRB in the sulfidogenic bioreactor after the treatment of acidic SMW (day 0–14), AMD (day 29–36), and JCW at COD/SO_4^{2-} ratios of 0.8 (day 14–29) and 1.4 (day 36–43). Averaged values of three samples taken from the top, middle, and bottom layers of the reactor with standard deviations are shown. Abbreviations: bacterial species (S), bacterial genus (G), bacterial family (F).

4. Discussion

Actual and synthetic MIWs were treated in a sulfidogenic up-flow biofilm reactor at low temperature. The SRRs achieved were far superior to others that have been reported for low-temperature SRB systems (Table 1) where the HRTs were relatively long in relation to the degree of sulfate removal achieved (Table 1). When higher sulfate concentrations were tested by Nevatalo et al. [20], the HRTs required were well in excess of those found in this research. According to Nielsen, SRR can increase over threefold as a result of a 10 °C increase in temperature [41]. However, the somewhat higher temperature in this study does not fully explain the higher SRR compared to those reported in other studies (Table 1). One reason for the high SRR is probably the carbon source used, as succinic acid is readily utilized by many species of SRB and the consortium was already acclimated to this electron donor in a previous study [22]. Ben Ali et al. also achieved a relatively efficient sulfate removal of almost 40% in 2.5 days using a complex carbon source consisting of wood chips and leaf compost [18]. In the present study, the reactor was operated at neutral pH, which is usually more suitable for most species of SRB. However, neutral pH conditions were also used by Sahinkaya et al. [19], Nevatalo et al. [20], and Nielsen et al. [13], but with inferior results.

The redox potentials (E_H) in the samples taken from the reactor remained relatively stable throughout the experiments. However, they fell to negative values when the actual MIWs were treated. The decrease in redox potential was probably due to the higher amount of inorganic reductants in the actual MIWs, i.e., metal ions and HS^- resulting from H_2S precipitation [42]. With the treatment of actual MIWs, the redox potential was lower with a higher operational pH, as expected. The solubility of transition metals is influenced by both the pH and E_H of the environment [43]. The chemical equilibrium calculations suggested that transition metals present in the MIWs would not have precipitated as sulfides nor as hydroxides at the measured E_H and operational pH. However, the precipitation of black metal sulfides was clearly detected when treating acidic SMW or JCW; according to the elemental analysis results of actual MIWs, metal concentrations were lower after the sulfate reduction process. Even though DeLaune and Reddy have stated that the optimal E_H for sulfate reduction is from –100 to –200 mV [44], E_H values higher than –100 mV in low temperature sulfate-reducing bioreactors have also been measured by Nielsen et al. [13] and Ben Ali et al. [18]. According to the chemical equilibrium calculations, the operational pH had a major effect on the H_2S/HS^- equilibrium inside the reactor. This was also detected as changes in the HRT. At a pH value of 7.00 and at 11.7 °C, approximately 60% of the sulfide-S was in the form of H_2S, and consumed H^+ ions increased the pH which consequently decreased the HRT. At a pH value of 7.50 and at 11.7 °C, approximately 70% of the produced sulfide-S was in the form of HS^-.

The initial pH of the actual MIWs was below 5 as most of the metals present in the waters, except trivalent Al and Fe, do not form hydroxide phases [10]. After precipitation with H_2S, the pH of the actual MIWs decreased to around 3 and mainly zinc precipitated as sulfide. The result was highly predictable, since zinc tends to precipitate as ZnS [33]. Most of the aluminum and iron in the actual MIWs was removed as hydroxides and oxides by filtration before the MIWs were fed into the reactor. The surface composition of the collected metal precipitates, revealed by XPS analysis, supports the results of the elemental analysis of precipitated MIWs as far as the metals present in high concentrations are concerned. In addition, the XRD data supports the XPS results of the precipitates collected from the H_2S-precipitated synthetic $CuSO_4$ solution and actual MIWs. The carbon detected by XPS in the precipitates collected after NaOH precipitation of AMD and H_2S precipitation of JCW is probably mostly that present in the actual MIWs used in the experiments.

The pH values of the sulfidogenic bioreactors varied between 7.00 and 7.50, causing both cobalt and nickel to precipitate. Due to the high S^{2-}/metal ratio inside the reactor, chemical speciation calculations made with the MINEQL+ program estimated that, under the operational

conditions, Co and Ni would precipitate as monosulfides. However, it must be noted that the presence of microorganisms and extracellular polymeric substances affect the phase of metal precipitates [45–47], which obviously cannot be taken into account in chemical speciation calculations. Metal sulfides precipitated with biologically produced sulfide-S in SRB cultivations have been analyzed by XRD in several studies, and the S^{2-}/metal ratio has been detected to have a great effect on the speciation of metals. Mansor et al. have reported precipitation of cobalt at pH 7.2 as CoS but also as cobalt pentlandite (Co_9S_8), and as cobalt-rich mackinawite ((Co,Fe)S) in the presence of iron [46]. NiS precipitation has been detected by Bijmans et al. [48], whereas Gramp et al. have reported precipitation of nickel only as heazlewoodite (Ni_3S_2) and vaesite (NiS_2) in the presence of SRB [49]. In this study, the chemical speciation calculations estimated that zinc would precipitate as ZnS inside the sulfidogenic bioreactor. The formation of ZnS has also been detected previously by Gramp et al. [49] and Xu et al. [47]. Gramp et al. reported the precipitation of iron as FeS and greigite (Fe_3S_4) in SRB cultivations, whereas FeS_2, which the chemical speciation calculations in this study estimated would be formed, was detected only in the absence of microorganisms [45]. In the study by Gramp et al., CuS was the only copper sulfide detected [50], whereas in this study the formation of $CuFeS_2$ was also estimated by the chemical speciation calculations when JCW containing high concentrations of iron was treated at pH 7.25 or 7.50.

According to the relative abundance of SRB, actual MIWs were more favorable for SRB than the SMW, which reflects the greater tolerance of the SRB to high concentrations of sulfate and metal (Fig. 5). However, it was also the case that actual MIWs were used as feed liquors after the acidic SMW, and the abundance of SRB increased over time. On the other hand, when acidic SMW was treated after the actual MIWs, no significant increase in SRR was detected. The actual MIWs were not sterilized before being fed into the reactor, which did not affect the species richness inside the reactor. In addition, the high COD/SO_4^{2-} ratio increased the relative abundance of SRB, but also increased the number of other bacteria, since species richness was highest after treatment at the COD/SO_4^{2-} ratio of 1.4. Bacterial numbers were highest in the middle of the bead layer, which can be explained by the reactor design: the bottom layer was impacted by oxygen due to the up-flow of fresh MIW, and most of the succinate was probably used by the time the feed migrated to the top liquid layer, which made the middle of the bead layer the most favorable zone for anaerobic bacteria.

Measurements of organic acids in the effluent liquors showed that succinate was metabolized completely, and that acetate was produced in stoichiometric amounts and not oxidized further by the SRB or the other microorganisms. Only at the COD/SO_4^{2-} ratio of 1.4 did the theoretical concentration of acetate exceed that of the measured concentration. With increasing ratios of organic carbon to sulfate, oxidation of proportionally less of the former is coupled to sulfate reduction and consequently less acetate is generated [51]. In addition to acetate, some propionate was formed inside the reactor. *Proteiniclasticum* sp., which was present in the reactor throughout the experiments, produces both acetate and propionate as fermentation products [52]. *Desulfobulbus propionicus* utilizes propionate as an electron donor and carbon source [53], while in the absence of sulfate *D. propionicus* can produce propionate as a fermentation product [54]. Since sulfate was present in the reactor all the time, it is unlikely that propionate was produced by *Desulfobulbus* sp., but it could have been utilized by the genus.

Halothiobacillus spp. and *Arcobacter sulfidicus* are known to oxidize sulfide to elemental sulfur [55,56], whereas *Geobacter sulfurreducens* is capable of reducing sulfur to sulfide [57]. The relative abundance of *Arcobacter* sp., *Geobacter* sp., and *Halothiobacillus* sp. was highest after the treatment of AMD, which could be explained by the operational pH used. The AMD was treated at pH values of 7.25–7.50, when the amount of soluble HS^- available for oxidation was higher compared to the operational pH of 7.00. Thus, the SRB consortium was adaptable to changes in growth conditions.

In this study, a 2 L sulfidogenic bioreactor with a liquid volume of 1.2 L was used for the treatment of mine waters with initial sulfate concentrations of 1600 mg L^{-1} (AMD) and 5350 mg L^{-1} (JCW). At the operational pH of 7.25 ± 0.10, 4.4 L d^{-1} of AMD was treated at the COD/SO_4^{2-} ratio of 0.8. At a pH value of 7.00 ± 0.10, 1.3 L d^{-1} of JCW was treated at the COD/SO_4^{2-} ratio of 1.4. Under the same operational conditions, with a 10 m^3 reactor, 22.15 m^3 d^{-1} and 6.25 m^3 d^{-1} of AMD and JCW could be treated, respectively. This would consume 33 kg d^{-1} and 57 kg d^{-1} succinate as a carbon source for AMD and JCW, respectively. According to the current market price of succinic acid, the cost of the carbon source would be \$66 d^{-1} and \$114 d^{-1} for the treatment of AMD and JCW, respectively. When considering the market prices of succinic acid and recoverable metals (Co, Cu, Fe, Ni, Zn), the operational costs of the reactor are not competitive. However, the costs of the carbon source would be covered multiple times if the water contained a higher amount of metals more valuable than iron [58]. Nevertheless, the primary target of the process is to treat the water so that it is clean enough to be discharged into the environment or reused at the mine site. A sulfidogenic bioreactor could be effectively used for treatment of moderate MIW flows.

As a next step, the reactor experiments could be scaled up to a pilot-scale field study where water quality and temperature conditions fluctuate to ensure the performance of the process in environmental conditions. For large MIW flows and high sulfate concentrations, the sulfidogenic bioreactor could be integrated with other methods, for example as a polishing step after gypsum precipitation. The method could also be tested for downstream processing of sulfate- and metals-containing rejects from membrane processes. However, finding a suitable treatment method is always dependent on water quality and the requirements for water purity.

5. Conclusions

A sulfidogenic bioreactor was successfully operated at neutral pH for the treatment of acidic mining-impacted waters at low temperature. The method proved to work well for the treatment of actual mining-impacted waters. A high sulfate feed and a high COD/SO_4^{2-} ratio increased the sulfate reduction rate and the relative abundance of sulfate-reducing bacteria. Further, some of the metals in the mining-impacted waters were removed extensively by hydrogen sulfide precipitation before the water was fed into the reactor, and the rest of the metals were precipitated inside the reactor vessel. In addition, sulfate reduction was highly predictable during the bioreactor experiment, and the bacterial consortium was found to be robust against changes in growth conditions.

Declaration of Competing Interest

The authors declare that they have no known competing financial interests or personal relationships that could have appeared to influence the work reported in this paper.

Acknowledgments

The study was conducted as part of the Comprehensive Sulphate Management in Cold Mining Wates (COSUMA) research project (Grant number 295050), funded by the Academy of Finland. The study was also part of the Supporting Environmental, Economic and Social Impacts of Mining Activity (KO1030 SEESIMA) research project and received financial support from the Kolarctic CBC (Cross-Border Collaboration), the European Union, Russia, Norway, Finland, and Sweden. Its contents are the sole responsibility of the authors at the University of Oulu, and do not necessarily reflect the views of the European Union or the participating countries. The authors wish to thank the Biocenter Oulu Sequencing Center for their 16S rRNA sequencing services.

Appendix A. Supplementary data

Supplementary data to this article can be found online at https://doi.org/10.1016/j.cej.2021.132050.

References

[1] M. Kumar, K. Pakshirajan, Novel insights into mechanism of biometal recovery from wastewater by sulfate reduction and its application in pollutant removal, Environ. Technol. Innov. 17 (2020), 100542, https://doi.org/10.1016/j.eti.2019.100542.

[2] D.B. Johnson, A.L. Santos, Biological removal of sulfurous compounds and metals from inorganic wastewaters, in: P.N.L. Lens (Ed.), Environmental Technologies to Treat Sulfur Pollution: Principles and Engineering, IWA Publishing, London, 2020, pp. 215–246, https://doi.org/10.2166/9781789060966_0215.

[3] T.P. Luoto, J.J. Leppänen, J. Weckström, Waste water discharge from a large Ni-Zn open cast mine degrades benthic integrity of Lake Nuasjärvi (Finland), Environ. Pollut. 255 (2019), 113268, https://doi.org/10.1016/j.envpol.2019.113268.

[4] H. Runtti, E. Tolonen, S. Tuomikoski, T. Luukkonen, U. Lassi, How to tackle the stringent sulfate removal requirements in mine water treatment—A review of potential methods, Environ. Res. 167 (2018) 207–222, https://doi.org/10.1016/j.envres.2018.07.018.

[5] E. Tolonen, T. Hu, J. Rämö, U. Lassi, The removal of sulphate from mine water by precipitation as ettringite and the utilisation of the precipitate as a sorbent for arsenate removal, J. Environ. Manage. 181 (2016) 856–862, https://doi.org/10.1016/j.jenvman.2016.06.053.

[6] A.M. Silva, R.M.F. Lima, V.A. Leão, Mine water treatment with limestone for sulfate removal, J. Hazard. Mater. 221–222 (2012) 45–55, https://doi.org/10.1016/j.jhazmat.2012.03.066.

[7] W. Chen, J. Mo, X. Du, Z. Zhang, W. Zhang, Biomimetic dynamic membrane for aquatic dye removal, Water Res. 151 (2019) 243–251, https://doi.org/10.1016/j.watres.2018.11.078.

[8] W. Zhang, F. Jiang, Membrane fouling in aerobic granular sludge (AGS)-membrane bioreactor (MBR): Effect of AGS size, Water Res. 157 (2019) 445–453, https://doi.org/10.1016/j.watres.2018.07.069.

[9] W. Zhang, W. Liang, Z. Zhang, T. Hao, Aerobic granular sludge (AGS) scouring to mitigate membrane fouling: Performance, hydrodynamic mechanism and contribution quantification model, Water Res. 188 (2021) 116518, https://doi.org/10.1016/j.watres.2020.116518.

[10] A.E. Lewis, Review of metal sulphide precipitation, Hydrometall. 104 (2) (2010) 222–234, https://doi.org/10.1016/j.hydromet.2010.06.010.

[11] A.H.M. Veeken, S. de Vries, A. van der Mark, W.H. Rulkens, Selective precipitation of heavy metals as controlled by a sulfide-selective electrode, Sep. Sci. Technol. 38 (1) (2003) 1–19, https://doi.org/10.1081/SS-120016695.

[12] D.B. Johnson, I. Sánchez-Andrea, Chapter Six - Dissimilatory reduction of sulfate and zero-valent sulfur at low pH and its significance for bioremediation and metal recovery, Adv. Microb. Physiol. 75 (2019) 205–231, https://doi.org/10.1016/bs.ampbs.2019.07.002.

[13] G. Nielsen, I. Hatam, K.A. Abuan, A. Janin, L. Coudert, J.F. Blais, G. Mercier, S. A. Baldwin, Semi-passive in-situ pilot scale bioreactor successfully removed sulfate and metals from mine impacted water under subarctic climatic conditions, Water Res. 140 (2018) 268–279, https://doi.org/10.1016/j.watres.2018.04.035.

[14] Natural Resources Canada, The Canadian Minerals and Metals Plan, Government of Canada, Ottawa, 2019.

[15] M. Tuusjärvi, I. Mäenpää, S. Vuori, P. Eilu, S. Kihlman, S. Koskela, Metal mining industry in Finland – development scenarios to 2030, J. Clean. Prod. 84 (2014) 271–280, https://doi.org/10.1016/j.jclepro.2014.03.038.

[16] R. Boyd, H. Gautneb, Mineral resources in Norway: potential and strategic importance, 2016 update, Trondheim, Norwegian Geological Survey (NGU), 2016.

[17] T.K. Tsukamoto, H.A. Killion, G.C. Miller, Column experiments for microbiological treatment of acid mine drainage: low-temperature, low-pH and matrix investigations, Water Res. 38 (6) (2004) 1405–1418, https://doi.org/10.1016/j.watres.2003.12.012.

[18] H.E. Ben Ali, C.M. Neculita, J.W. Molson, A. Maqsoud, G.J. Zagury, Salinity and low temperature effects on the performance of column biochemical reactors for the treatment of acidic and neutral mine drainage, Chemosphere 243 (2020) 125303, https://doi.org/10.1016/j.chemosphere.2019.125303.

[19] E. Sahinkaya, B. Özkaya, A.H. Kaksonen, J.A. Puhakka, Sulfidogenic fluidized-bed treatment of metal-containing wastewater at low and high temperatures, Biotechnol. Bioeng. 96 (6) (2007) 1064–1072, https://doi.org/10.1002/bit.21195.

[20] L.M. Nevatalo, M.F.M. Bijmans, P.N.L. Lens, A.H. Kaksonen, J.A. Puhakka, The effect of sub-optimal temperature on specific sulfidogenic activity of mesophilic SRB in an H2-fed membrane bioreactor, Process Biochem. 45 (3) (2010) 363–368, https://doi.org/10.1016/j.procbio.2009.10.007.

[21] I. Nancucheo, D.B. Johnson, Selective removal of transition metals from acidic mine waters by novel consortia of acidophilic sulfidogenic bacteria, Microb. Biotechnol. 5 (2012) 34–44, https://doi.org/10.1111/j.1751-7915.2011.00285.x.

[22] H. Virpiranta, S. Taskila, T. Leiviskä, J. Rämö, J. Tanskanen, Development of a process for microbial sulfate reduction in cold mining waters – Cold acclimation of bacterial consortia from an Arctic mining district, Environmental Pollution 252 (2019) 281–288, https://doi.org/10.1016/j.envpol.2019.05.087.

[23] D.T. Sawyer, A. Sobkowiak, J.L. Roberts, Electrochemistry for Chemists, second ed., John Wiley & Sons Inc, New York, 1995.

[24] W.D. Schecher, D.C. McAvoy, MINEQL+: A Chemical Equilibrium Modeling System, Version 5.0 for Windows, User's Manual, Environmental Research Software, Hallowell, 2015.

[25] QIAGEN, DNeasy PowerSoil Kit Handbook, QIAGEN, Hilden, 2017.

[26] V. Krylova, M. Andrulevičius, Optical, XPS and XRD Studies of Semiconducting Copper Sulfide Layers on a Polyamide Film, Int. J. Photoenergy 2009 (2009) 1–8, https://doi.org/10.1155/2009/304308.

[27] M.C. Biesinger, Advanced analysis of copper X-ray photoelectron spectra, Surf. Interface Anal. 49 (2017) 1325–1334, https://doi.org/10.1002/sia.6239.

[28] C. Falagán, I. Yusta, J. Sánchez-España, D.B. Johnson, Biologically-induced precipitation of aluminium in synthetic acid mine water, Minerals Eng. 106 (2017) 79–85, https://doi.org/10.1016/j.mineng.2016.09.028.

[29] Y. Zhang, Y. Jia, Fluoride adsorption onto amorphous aluminum hydroxide: Roles of the surface acetate anions, J. Colloid Interface Sci. 483 (2016) 295–306, https://doi.org/10.1016/j.jcis.2016.08.054.

[30] W. Gong, J. Qu, R. Liu, H. Lan, Effect of aluminum fluoride complexation on fluoride removal by coagulation, Colloids Surf. Physicochem. Eng. Aspects 395 (2012) 88–93, https://doi.org/10.1016/j.colsurfa.2011.12.010.

[31] J. Duchoslav, R. Steinberger, M. Arndt, D. Stifter, XPS study of zinc hydroxide as a potential corrosion product of zinc: Rapid X-ray induced conversion into zinc oxide, Corros. Sci. 82 (2014) 356–361, https://doi.org/10.1016/j.corsci.2014.01.037.

[32] P.F. Teh, Synthesis and electrochemical performance of transition metal oxide anodes in lithium ion batteries, Nanyang Technological University, Singapore, 2013.

[33] S. Al-Abed, P.X. Pinto, J. McKernan, E. Feld-Cook, S.M. Lomnicki, Mechanisms and effectivity of sulfate reducing bioreactors using a chitinous substrate in treating mining influenced water, Chem. Eng. J. 323 (2017) 270–277, https://doi.org/10.1016/j.cej.2017.04.045.

[34] B. Abdallah, HRTEM, XPS and XRD characterization of ZnS/PbS nanorods prepared by thermal evaporation technique, Nanosyst. Phys. Chem. Math. 11 (2020) 1–9.

[35] T. Leiviskä, J. Matusik, B. Muir, J. Tanskanen, Vanadium removal by organo-zeolites and iron-based products from contaminated natural water, J. Clean. Prod. 167 (2017) 589–600, https://doi.org/10.1016/j.jclepro.2017.08.209.

[36] A.D. Parker, Oxidative Dissolution of Chalcopyrite in Ferric Media: An X-ray Photoelectron Spectroscopy Study, Curtin University of Technology, Perth, 2008.

[37] E.A. Deliyanni, L. Nalbandian, K.A. Matis, Adsorptive removal of arsenites by a nanocrystalline hybrid surfactant–akaganeite sorbent, J. Colloid Interface Sci. 302 (2) (2006) 458–466, https://doi.org/10.1016/j.jcis.2006.07.007.

[38] A. Al-Anazi, W.H. Abdelraheem, C. Han, M.N. Nadagouda, L. Sygellou, M. K. Arfanis, P. Falaras, V.K. Sharma, D.D. Dionysiou, Cobalt ferrite nanoparticles with controlled composition-peroxymonosulfate mediated degradation of 2-phenylbenzimidazole-5-sulfonic acid, Appl. Catal. B: Environ. 221 (2018) 266–279, https://doi.org/10.1016/j.apcatb.2017.08.054.

[39] R. Barik, B.K. Jena, M. Mohapatra, Metal doped mesoporous FeOOH nanorods for high performance supercapacitors, RSC Adv. 7 (77) (2017) 49083–49090, https://doi.org/10.1039/C7RA06731C.

[40] R. Demir-Cakan, M. Morcrette, F. Nouar, C. Davoisne, T. Devic, D. Gonbeau, R. Dominko, C. Serre, G. Férey, J.-M. Tarascon, Cathode Composites for Li–S Batteries via the Use of Oxygenated Porous Architectures, J. Am. Chem. Soc. 133 (40) (2011) 16154–16160, https://doi.org/10.1021/ja2062659.

[41] P.H. Nielsen, Biofilm Dynamics and Kinetics during High-Rate Sulfate Reduction under Anaerobic Conditions, Appl. Environ. Microbiol. 53 (1) (1987) 27–32.

[42] J. Dolfing, M. van Eekert, J. Mueller, Thermodynamics of low Eh reactions, Battelle Memorial Institute, Monterey, 2006.

[43] L. Choudhary, D.D. Macdonald, A. Alfantazi, Role of Thiosulfate in the Corrosion of Steels: A Review, Corros. 71 (9) (2015) 1147–1168, https://doi.org/10.5006/1709.

[44] R.D. DeLaune, K.R. Reddy, 284. Redox Potential, in: D. Hillel (Ed.), Encyclopedia of Soils in the Environment, Academic Press, Cambridge, 2005, pp. 366–371.

[45] J.P. Gramp, J.M. Bigham, F.S. Jones, O.H. Tuovinen, Formation of Fe-sulfides in cultures of sulfate-reducing bacteria, J. Hazard. Mater. 175 (1–3) (2010) 1062–1067, https://doi.org/10.1016/j.jhazmat.2009.10.119.

[46] M. Mansor, E. Cantando, Y. Wang, J.A. Hernandez-Viezcas, J.L. Gardea-Torresdey, M.F. Hochella, J. Xu, Insights into the Biogeochemical Cycling of Cobalt: Precipitation and Transformation of Cobalt Sulfide Nanoparticles under Low-Temperature Aqueous Conditions, Environ. Sci. Technol. 54 (9) (2020) 5598–5607, https://doi.org/10.1021/acs.est.0c01363.

[47] J. Xu, M. Murayama, C.M. Roco, H. Veeramani, F.M. Michel, J.D. Rimstidt, C. Winkler, M.F. Hochella, Highly-defective nanocrystals of ZnS formed via dissimilatory bacterial sulfate reduction: A comparative study with their abiogenic analogues, Geochim. Cosmochim. Acta 180 (2016) 1–14, https://doi.org/10.1016/j.gca.2016.02.007.

[48] M.F.M. Bijmans, P.-J. van Helvoort, S.A. Dar, M. Dopson, P.N.L. Lens, C.J. N. Buisman, Selective recovery of nickel over iron from a nickel–iron solution using microbial sulfate reduction in a gas-lift bioreactor, Water Res. 43 (3) (2009) 853–861, https://doi.org/10.1016/j.watres.2008.11.023.

[49] J.P. Gramp, J.M. Bigham, K. Sasaki, O.H. Tuovinen, Formation of Ni- and Zn-Sulfides in Cultures of Sulfate-Reducing Bacteria, Geomicrobiol. J. 24 (7–8) (2007) 609–614, https://doi.org/10.1080/01490450701758239.

[50] J.P. Gramp, K. Sasaki, J.M. Bigham, O.V. Karnachuk, O.H. Tuovinen, Formation of Covellite (CuS) Under Biological Sulfate-Reducing Conditions, Geomicrobiol. J. 23 (8) (2006) 613–619, https://doi.org/10.1080/01490450600964383.

[51] Y. Zhao, N. Ren, A. Wang, Contributions of fermentative acidogenic bacteria and sulfate-reducing bacteria to lactate degradation and sulfate reduction,

Chemosphere 72 (2) (2008) 233–242, https://doi.org/10.1016/j.chemosphere.2008.01.046.
[52] K. Zhang, L. Song, X. Dong, Proteiniclasticum ruminis gen. nov., sp. nov., a strictly anaerobic proteolytic bacterium isolated from yak rumen, Int. J. Syst. Evolut. Microbiol. 60 (2010) 2221–2225, https://doi.org/10.1099/ijs.0.011759-0.
[53] F. Widdel, N. Pfennig, Studies on dissimilatory sulfate-reducing bacteria that decompose fatty acids II. Incomplete oxidation of propionate by Desulfobulbus propionicus gen. nov., sp. nov., Arch. Microbiol. 131 (1982) 360-365.
[54] M. Tasaki, Y. Kamagata, K. Nakamura, K. Okamura, K. Minami, Acetogenesis from pyruvate by Desulfotomaculum thermobenzoicum and differences in pyruvate metabolism among three sulfate-reducing bacteria in the absence of sulfate, FEMS Microbiol. Lett. 106 (1993) 259–263, https://doi.org/10.1111/j.1574-6968.1993.tb05973.x.
[55] C.O. Wirsen, S.M. Sievert, C.M. Cavanaugh, S.J. Molyneaux, A. Ahmad, L.T. Taylor, E.F. DeLong, C.D. Taylor, Characterization of an Autotrophic Sulfide-Oxidizing Marine Arcobacter sp. That Produces Filamentous Sulfur, Appl. Environ. Microbiol. 68 (2002) 316-325. https://doi.org/10.1128/AEM.68.1.316-325.2002.
[56] K. Whaley-Martin, G.L. Jessen, T.C. Nelson, J.F. Mori, S. Apte, C. Jarolimek, L. A. Warren, The Potential Role of Halothiobacillus spp. in Sulfur Oxidation and Acid Generation in Circum-Neutral Mine Tailings Reservoirs, Front. Microbiol. 10 (2019) 297, https://doi.org/10.3389/fmicb.2019.00297.
[57] F Caccavo, D J Lonergan, D R Lovley, M Davis, J F Stolz, M J McInerney, Geobacter sulfurreducens sp. nov., a hydrogen- and acetate-oxidizing dissimilatory metal-reducing microorganism, Appl. Environ. Microbiol. 60 (10) (1994) 3752–3759.
[58] A.L. Santos, D.B. Johnson, Design and Application of a Low pH Upflow Biofilm Sulfidogenic Bioreactor for Recovering Transition Metals From Synthetic Waste Water at a Brazilian Copper Mine, Front. Microbiol. 9 (2018) 2051.